A novel auxin-inducible degron system for rapid, cell cycle-specific targeted proteolysis

Dario Palmieri (dario.palmieri@osumc.edu)
The Ohio State University https://orcid.org/0000-0002-0797-4268
Marina Capece
The Ohio State University
Anna Tessari
The Ohio State University
Joseph Mills
The Ohio State University
Gian Luca Rampioni Vinciguerra
The Ohio State University
Chenyu Lin
The Ohio State University
Bryan McElwain
The Ohio State University
Wayne Miles
The Ohio State University
Vincenzo Coppola
The Ohio State University https://orcid.org/0000-0001-6163-1779
Carlo Croce
The Ohio State University

Brief Communication

Keywords:

Posted Date: May 10th, 2022

DOI: https://doi.org/10.21203/rs.3.rs-584199/v1

Abstract

The OsTIR1/auxin-inducible degron (AID) system allows selective protein degradation upon exposure to the phytohormone auxin. However, this technology does not allow to study the effect of acute protein depletion selectively in one phase of the cell cycle. Here, we report a new AID system to Regulate OsTIR1 Levels based on the Cell Cycle Status (ROLECCS) for phase-specific target proteolysis. Finally, we applied the ROLECCS technology to show that the tumor suppressor TP53 plays a S/G2-specific role in suppression of micronuclei accumulation. This new tool allows the analysis of different protein functions during cell cycle progression with unprecedented temporal resolution.

Main Text

Despite the advancements of genetic tools such as CRISPR/Cas9-based gene editing[1], gene silencing[2], or inducible gene expression approaches[3], none of these systems displays readiness of activity compatible with the kinetics of cell cycle progression. Conversely, an alternative to obtain rapid degradation of the POI is represented by targeted proteolysis using polypeptide tags, also known as degrons[4,5]. In one of the most commonly used degron systems, the POI is fused with an Auxin-Inducible Degron (AID) sequence, such as the 7 kDa degron termed mini-AID (mAID), in cell lines expressing the *Oryza sativa* TIR1 (*Os*TIR1) F-box protein[6,7]. When the phytohormone auxin is provided, OsTIR1 binds the mAID-POI and induces its quick proteasomal degradation[6,7]. However, despite their speed, reversibility, and fine-tuning, degron-based systems still lack cell cycle phase-specificity and require conventional cell synchronization[8], routinely achieved by exposing cells to stress conditions[9,10].

Here, we report the engineering of the “Regulated OsTIR1 Levels of Expression based on the Cell-Cycle Status” (ROLECCS) technology, which combines the AID and the FUCCI systems. In this new tool, the *Os*TIR1 protein is fused to the fluorescent indicator mEmerald and the FUCCI[11] tags Cdt1/Geminin, which are responsible for the restricted G_1 and S/G_2 expression, respectively. Upon auxin treatment, only the cells expressing the fusion-protein OsTIR1-mEmerald-Cdt1/Geminin, (i.e. in the desired cell cycle phase) degrade the mAID-POI.

In our design (**Figure 1A-C, Supplementary Figure 1A**), the OsTIR1 coding gene was fused in-frame with a mEmerald fluorescent reporter (a brightly fluorescent monomeric variant of GFP)[12] that allows the identification of cells expressing these constructs. Then, we added the sequences corresponding to either human Cdt1 (aa 30-120) or Geminin (aa 1-110) to restrict OsTIR1 expression to different phases of the cell cycle, like in the FUCCI system. For convenience, the hCdt1 (30-120) and hGeminin (1-110) tags are indicated hereafter as Cdt1 and GEM, respectively. We also generated a construct where no additional tag was added, to allow OsTIR1-mEmerald expression independently on the phase of the cell cycle.

Engineered variants of OsTIR1-mEmerald, OsTIR1-mEmerald-Cdt1, and OsTIR1-mEmerald-GEM genes are actively transcribed throughout the cell cycle. However, the presence of the Cdt1 and the Geminin tags determine the Regulated OsTIR1 Levels of Expression based on the Cell Cycle Status (ROLECCS system).

We predicted that the OsTIR1-mEmerald protein would be stably present throughout the cell cycle. Therefore, auxin treatment would trigger OsTIR1 enzymatic activity and degradation of the mAID-tagged protein of interest in any cell, independent of the cell cycle status (from now on: asynchronous ROLECCS, ROLECCS AS) (**Figure 1A**).

On the other hand, the presence of OsTIR1-mEmerald-Cdt1 (from now on: ROLECCS G1) protein would be restricted the G_1/early S phase, because ubiquitylation by SCF^{Skp2} E3 ligase leads to its prompt degradation during S-phase transition. Thus, addition of auxin would lead to OsTIR1-mediated proteasomal degradation of the POI exclusively in those cells in G_1/S phase during the treatment (**Figure 1B**).

Similarly, presence of OsTIR1-mEmerald-GEM (from now on: ROLECCS G2) protein would be restricted during the late S-G_2-M phase, peaking during the G_2, as APC^{Cdh1}-mediated ubiquitylation and degradation is rapidly triggered during M/G_1 transition. Consequently, auxin treatment would cause degradation of the POI exclusively in cells going through the late S-G_2-M phase of the cell cycle during the treatment (**Figure 1C**).

Each ROLECCS construct was abundantly expressed both transiently (at 72h from transfection) and stably (after *AAVS1* knock-in) in HEK293 cells (**Supplementary Figure 1B-D**), both in the nucleus and in the cytoplasm of transfected cells. Live cell imaging was performed on ROLECCS AS, G1 and G2 knock-in HEK-293 to monitor the green fluorescence in real time. **Figure 1D** (top) and **Supplementary Video 1** show that ROLECCS AS expression did not change during a full cell cycle. Conversely ROLECCS G1 was not visible in actively dividing cells (**Figure 1D, middle and Supplementary Video 2**), becoming detectable immediately upon completion of cell division. Finally, ROLECCS G2 was visible only in actively dividing cells, with the fluorescence intensity peaking at G_2/M transition (**Figure 1D, bottom and Supplementary Video 3**).

To orthogonally validate ROLECCS G1 and ROLECCS G2 as cell cycle indicators, we sorted *AAVS1*-integrated ROLECCS HEK-293 based on their green fluorescence level and cellular complexity, as described in the methods section. GFP^{high}-sorted ROLECCS G1 population mostly comprised cells in the G_1/early S phase (94.6±1.6%), in comparison with GFP^{med} and GFP^{low} sorted populations (67.7±9.4% and 26.9±12.2% respectively) (**Figure 1E-F**). Conversely, GFP^{high} ROLECCS G2 population showed a significant enrichment in late S/G_2 phase cells (74.64±5%), compared to GFP^{med} and GFP^{low} sorted cells (28.8±7.2% and 3.5±1.5%, respectively) (**Figure 1G-H**). Conversely, unsorted ROLECCS G1 and ROLECCS G2 populations displayed cell cycle distribution typical of unsynchronized HEK-293 cells.

To assess that the enzymatic activity of OsTIR1-containing SCF complexes was not hampered by the mEmerald-Cdt1 and mEmerald-GEM tags of the ROLECCS G1 and G2, we transiently transfected *AAVS1*-integrated ROLECCS AS, ROLECCS G1, and ROLECCS G2 HEK-293 cells with a mAID-mCherry fluorescent reporter and measured its protein levels upon auxin treatment. mAID-mCherry levels were appreciably

reduced upon auxin treatment when performed at 8h after reporter vector transfection, indicating that the biological activity of OsTIR1 was preserved (**Supplementary Figure 1E**). We hypothesized that an overexpressed target could be efficiently degraded only if the molar ratio between the POI and the ROLECCS was favorable to the latter, as in the very first hours (<8h) after transfection. Accordingly, other groups have generated All-in-One systems to achieve equimolar levels of OsTIR1 and its targets[13].

As shown in **Supplementary Figure 2A-B**, we created 3 all-in-one lentiviral vectors (pLentiROLECCS AS, G1, and G2) in which the ROLECCS proteins were fused with mAID-mCherry using an autoproteolytic P2A sequence[14].

Next, we treated HEK-293 cells stably expressing LentiROLECCS G1 or LentiROLECCS G2 with auxin for 1h. Cells were sorted based on their GFP fluorescence intensity and SSC (**Supplementary Figure 3A-D**). Red fluorescent intensity (from mAID-mCherry) was simultaneously quantified on GFP^{low}, GFP^{med}, and GFP^{high} populations. **Supplementary Figures 4A-B** show that downregulation of the mCherry fluorescence was specifically achieved in GFP^{med} and GFP^{high} populations upon auxin treatment.

Western blot analysis confirmed that GFP^{med} and GFP^{High} sorted cell populations expressed the highest levels of ROLECCS G1 and ROLECCS G2 (**Figure 1I-J** and **Supplementary Figure 4C-F**). Notably, highest levels of ROLECCS G1 corresponded to highest expression of Cdt1 (a G_1-specific marker, frequently identified as a doublet corresponding to Cdt1/phosphoCdt1[15]) and to the lowest levels of Cyclin B1 (a late-S/G_2 marker). Importantly, downregulation of the target mAID-mCherry was only observed in sorted GFP^{high} ROLECCS G1 cells upon auxin treatment, and not in the untreated or GFP^{low} auxin-treated controls. Differently, ROLECCS G2 accumulation was observed in cell populations displaying highest levels of Cyclin B1 and lowest levels of Cdt1, but target downregulation was still only observed upon auxin treatment.

Taken together, our data indicate that the ROLECCS system allows temporally-restricted selective degradation of mAID-tagged targets based on the cell cycle phase.

Then, we decided to test whether the ROLECCS system could accomplish the cell cycle phase-specific downregulation of an endogenous target such as TP53, a well-known transcriptional factor playing a central role in the control of cell cycle progression, especially in response to DNA-damaging agents[16,17].

First, we generated HCT116 cell lines where both wild-type *TP53* alleles were modified by CRISPR/Cas9-mediated knock-in (HCT116 TP53-mAID-mCherry). For gene editing purposes, the stop codon of the endogenous *TP53* gene was replaced by a mAID-mCherry fusion cassette (as described in Methods section) (**Supplementary Figure 5A-D**).

Western blot analysis showed that gene-edited TP53 had a marked molecular size increase (final predicted molecular weight ~87KDa, compared to WT TP53, 53KDa), due to the presence of the mAID and mCherry tags. Importantly, gene-edited TP53 was still upregulated by DNA damaging agents such as

cisplatin treatment, and its nuclear and cytoplasmic localization followed the expected distribution pattern[16,17] (**Supplementary Figure 5E**).

Next, we further edited HCT116 TP53-mAID-mCherry cells inserting the ROLECCS constructs in the *AAVS1* safe harbor site, generating HCT116 TP53-mAID-mCherry ROLECCS cell lines (**Figure 2A**). As shown in **Figure 2B**, sustained expression of ROLECCS AS, G1, and G2 with the expected molecular weight was achieved in at least 2 independent clones. Since this analysis was performed on asynchronously growing HCT116 TP53-mAID-mCherry ROLECCS cells, the three ROLECCS constructs apparently displayed different expression levels. However, these differences are likely due to the fact that ROLECCS G1 and ROLECCS G2 are expressed only in phase-specific cell subpopulations, while ROLECCS AS is equally expressed throughout the cell cycle. Nonetheless, since we did not perform relative comparisons between ROLECCS AS and ROLECCS G1 or G2, these differences did not affect downstream analyses. We also noticed a mild reduction in the levels of edited TP53 in comparison with parental HCT116 cells, compatible with the partial leakiness observed for the AID system[18,19]. For this reason, for all the functional studies, cells were pre-treated with auxinole. a previously-reported inhibitor of OsTIR1[18], to neutralize the activity of the ROLECCS system in the absence of auxin.

Finally, we treated HCT116 TP53-mAID-mCherry ROLECCS G1 and G2 cells with auxin. At 1h after auxin treatment, cells were sorted (**Supplementary Figure 6A-D**) as described in the Methods section. As shown in **Figure 2C-D**, TP53 downregulation was noticeable in unsorted populations both in ROLECCS G1- and G2-expressing cells. However, upon sorting, we observed that TP53 downregulation upon auxin treatment was only achieved in GFP^{med} and GFP^{high} sorted populations, in comparison with GFP^{low} cells for both ROLECCS constructs. Importantly, Cdt1 and Cyclin B1 levels confirmed that ROLECCS G1 GFP^{med} and GFP^{high} represented a cell population enriched in G_1/early S phase of the cell cycle. On the other hand, ROLECCS G2 GFP^{med} and GFP^{high} cells were mostly representing cells in the late S/G_2 phase. Similar results were obtained using two independent clones for each ROLECCS protein (**Supplementary Figure 7A-D**). These data indicate that the ROLECCS system can be used to achieve the phase-specific downregulation of an endogenous target, appropriately gene edited to include a mAID tag (**Figure 2E**).

Protein biological functions and cell cycle progression are intimately connected and reciprocally affected. Hence, the cell cycle status should be taken into account for the study of any biological phenomenon. Thanks to its phase specificity, rapidity, reversibility, and low overall perturbation of other biological processes, the ROLECCS technology represents a unique tool for the investigation of biological phenomena and their relationship with the cell cycle progression.

Methods

A detailed description of the methods used for the study is reported in the Supplementary Information file.

Declarations

Acknowledgements

We thank Dr. Emanuele Cocucci for the scientific discussions during the preparation of this manuscript. We also thank the countless investigators who made their plasmids and reagents available through public repositories such as Addgene. This work was supported by seed funds from The Ohio State University Comprehensive Cancer Center (DP, CMC), Pelotonia (DP) and NCI-NIH (NIH R35CA197706) (CMC). The Gene Editing Shared Resource, the Flow Cytometry Shared Resource and the Genomics Shared Resource that contributed to this study are supported by the Cancer Center Support Grant P30CA016058.

Author Contributions

M.C., D.P. and C.M.C. conceived and designed the project. M.C., D.P., A.T., W.O.M. conceived and planned the experiments. M.C., D.P., A.T., J.M., G.L.R.V., C.L., W.O.M. executed the experiments. M.C., D.P., A.T., G.L.R.V., C.L., W.O.M. analyzed the data. B.M. provided technical support for flow cytometry experiments and cell sorting. M.C. and D.P., wrote the manuscript. A.T., J.M., G.L.R.V., C.L., W.O.M., V.C. and C.M.C. provided critical feedback and contributed to the final version of the manuscript.

References

1. Anzalone, A. V., Koblan, L. W. & Liu, D. R. Genome editing with CRISPR–Cas nucleases, base editors, transposases and prime editors. *Nature Biotechnology* vol. 38 824–844 (2020).

2. Ashfaq, M. A. *et al.* Post-transcriptional gene silencing: Basic concepts and applications. *Journal of Biosciences* vol. 45 1–10 (2020).

3. Kallunki, T., Barisic, M., Jäättelä, M. & Liu, B. How to Choose the Right Inducible Gene Expression System for Mammalian Studies? *Cells* vol. 8 (2019).

4. Yesbolatova, A. *et al.* The auxin-inducible degron 2 technology provides sharp degradation control in yeast, mammalian cells, and mice. *Nat. Commun.* **11**, 1–13 (2020).

5. Röth, S., Fulcher, L. J. & Sapkota, G. P. Advances in targeted degradation of endogenous proteins. *Cellular and Molecular Life Sciences* vol. 76 2761–2777 (2019).

6. Natsume, T., Kiyomitsu, T., Saga, Y. & Kanemaki, M. T. Rapid Protein Depletion in Human Cells by Auxin-Inducible Degron Tagging with Short Homology Donors. *Cell Rep.* **15**, 210–218 (2016).

7. H Nishimura, M. N. H. H. N. M. T. H. Development of lupus-like autoimmune diseases by disruption of the PD-1 gene encoding an ITIM motif-carrying immunoreceptor. *Immunity* **11**, 141–151 (1999).

8. Hoffmann, S. & Fachinetti, D. Real-Time De Novo Deposition of Centromeric Histone-Associated Proteins Using the Auxin-Inducible Degradation System. in *Methods in Molecular Biology* vol. 1832 223–241 (Humana Press Inc., 2018).

9. Schorl, C. & Sedivy, J. M. Analysis of cell cycle phases and progression in cultured mammalian cells. *Methods* **41**, 143–150 (2007).

10. Uzbekov, R. E. Analysis of the cell cycle and a method employing synchronized cells for study of protein expression at various stages of the cell cycle. *Biochemistry (Moscow)* vol. 69 485–496 (2004).

11. Sakaue-Sawano, A. *et al.* Genetically Encoded Tools for Optical Dissection of the Mammalian Cell Cycle. *Mol. Cell* **68**, 626-640.e5 (2017).

12. Chudakov, D. M., Matz, M. V., Lukyanov, S. & Lukyanov, K. A. Fluorescent proteins and their applications in imaging living cells and tissues. *Physiol. Rev.* **90**, 1103–1163 (2010).

13. Yesbolatova, A., Saito, Y. & Kanemaki, M. T. Constructing auxin-inducible degron mutants using an all-in-one vector. *Pharmaceuticals* **13**, (2020).

14. Kim, J. H. *et al.* High Cleavage Efficiency of a 2A Peptide Derived from Porcine Teschovirus-1 in Human Cell Lines, Zebrafish and Mice. *PLoS One* **6**, e18556 (2011).

15. Liu, E., Li, X., Yan, F., Zhao, Q. & Wu, X. Cyclin-dependent Kinases Phosphorylate Human Cdt1 and Induce Its Degradation. *J. Biol. Chem.* **279**, 17283–17288 (2004).

16. Vousden, K. H. & Lane, D. P. p53 in health and disease. *Nature Reviews Molecular Cell Biology* vol. 8 275–283 (2007).

17. Kastenhuber, E. R. & Lowe, S. W. Putting p53 in Context. *Cell* vol. 170 1062–1078 (2017).

18. Yesbolatova, A., Natsume, T., Hayashi, K. ichiro & Kanemaki, M. T. Generation of conditional auxin-inducible degron (AID) cells and tight control of degron-fused proteins using the degradation inhibitor auxinole. *Methods* **164–165**, 73–80 (2019).

19. Li, S., Prasanna, X., Salo, V. T., Vattulainen, I. & Ikonen, E. An efficient auxin-inducible degron system with low basal degradation in human cells. *Nat. Methods* **16**, 866–869 (2019).

Figures

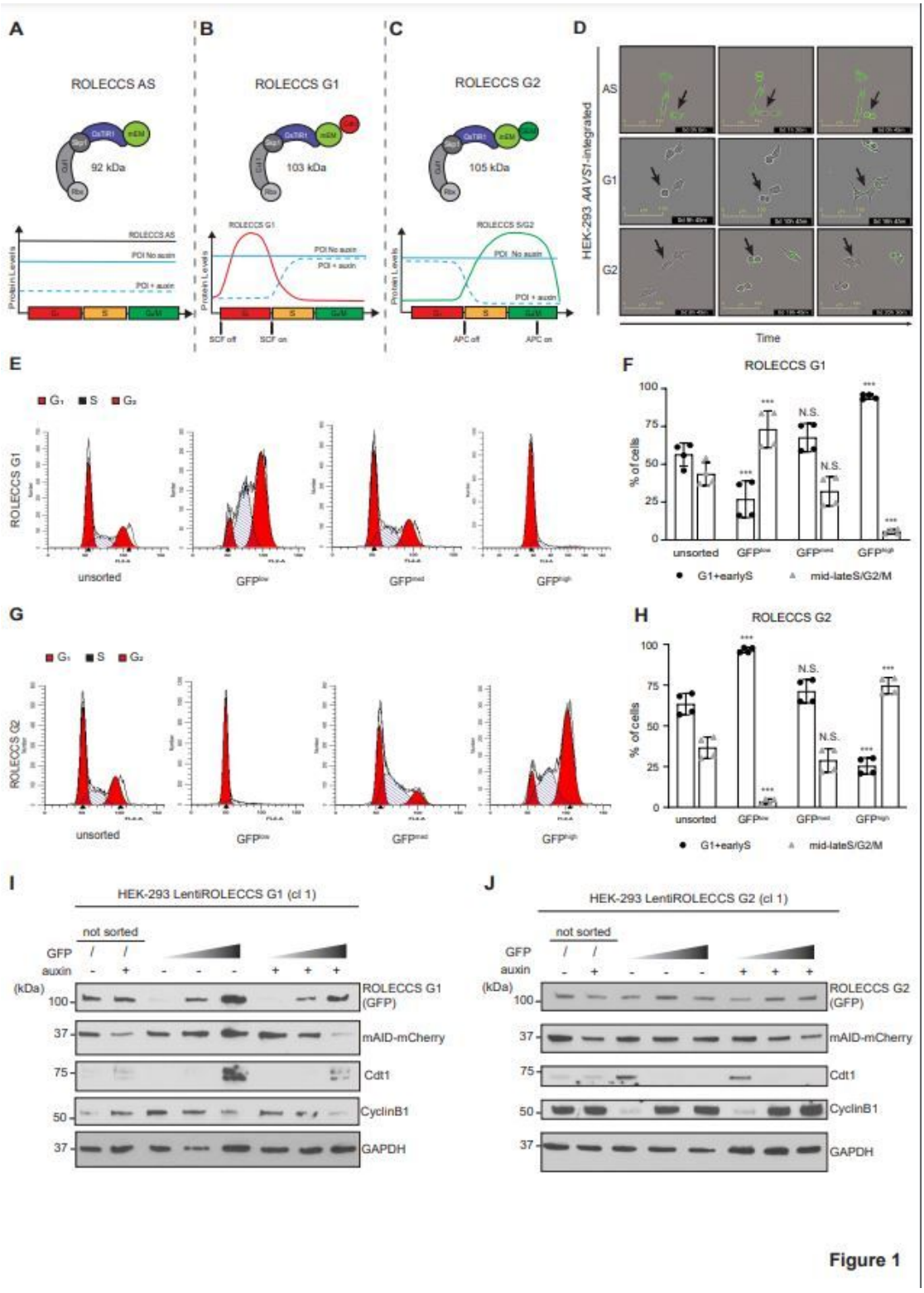

Figure 1

Expression of Regulated OsTIR1 Levels of Expression based on the Cell Cycle Status (ROLECCS) variants (ROLECCS AS, G1, and G2) during cell-cycle progression and their biological activity. (**A**) OsTIR1-mEmerald protein (asynchronous ROLECCS, ROLECCS AS, 92 KDa) is stably expressed throughout the cell cycle. Upon auxin treatment, OsTIR1 enzymatic activity elicits the degradation of the mAID-tagged protein of interest (POI) in any cell, independently of the cell cycle status. (**B**) The expression of the

ROLECCS G1 variant (OsTIR1-mEmerald-Cdt1, 103 KDa) is restricted to the G_1/early S phase by the presence of the Cdt1 tag, when the SCF^{Skp2} E3 ligase activity is off. This, in turn, leads to auxin-dependent ubiquitylation and proteasome degradation of mAID-tagged POIs. In cells transitioning during S, G_2 and M phases, SCF^{Skp2} activity is naturally restored, leading to ROLECCS G1 degradation by ubiquitylation, and stabilization of the POI even in the presence of auxin. (**C**) The Geminin tag of the ROLECCS G2 variant (OsTIR1-mEmerald-GEM, 105 KDa) ensures its restricted expression during the late S-G_2-M phase, as APC^{Cdh1}-mediated ubiquitylation and degradation is rapidly triggered during M/G_1 transition. Therefore, auxin treatment induces degradation of the POI exclusively in cells going through the late S-G_2-M phase of the cell cycle. (**D**) Time-frame pictures of duplicating HEK-293 *AAVS1*-integrated clones. Note the cell cycle-dependent changes in fluorescence of specific ROLECCS variants (AS, G1, G2) (green). Arrows indicate cells that are completing a cell cycle. (**E** and **G**) Cell-cycle distribution histograms of HEK-293 *AAVS1*-integrated clones expressing ROLECCS G1 and G2, obtained by propidium iodide staining and flow cytometry analysis. Red peaks indicate G1 and G2 phase, stripes indicate S phase. Cells were prior sorted based on GFP levels (GFP^{low}, GFP^{med}, GFP^{high}), as described in Supplementary Figure 3. Not sorted (unsorted) populations are reported for comparison. Data are representative of four independent experiments. (**F** and **H**) Quantification of experiments reported in E and G. GFP^{low}, GFP^{med}, GFP^{high} subpopulations were analyzed for cells composition as percentage of cells in G_1+earlyS and cells in mid-lateS/G_2/M, using ModFit software v5.0. Error bars indicate mean ± SD. *** $p < 0.001$, N.S. not significant. Statistics (two-tailed t-test) is calculated *versus* respective unsorted populations. Data are the average of four independent experiments. (**I**) WB analysis of HEK-293 cells transfected with pLentiROLECCS G1, (clone 1, cl 1) after sorting. Cells were treated with auxin or left untreated for one hour and then sorted based on increasing GFP intensity (ascending grey gradient triangle). Membrane was probed with anti-GFP antibody for ROLECCS G1 detection and mCherry antibody for mAID-mCherry detection. Cdt1 and CyclinB1 were used as G_1 phase and G_2 phase specific markers, respectively. GAPDH was used as loading control. Not sorted (unsorted) cells were loaded for comparison. (**J**) WB analysis of HEK-293 cells transfected with pLentiROLECCS G2 (clone 1, cl 1), after sorting. Treatments, sorting and antibodies were performed as in G. Blots are representative of at least two independent experiments.

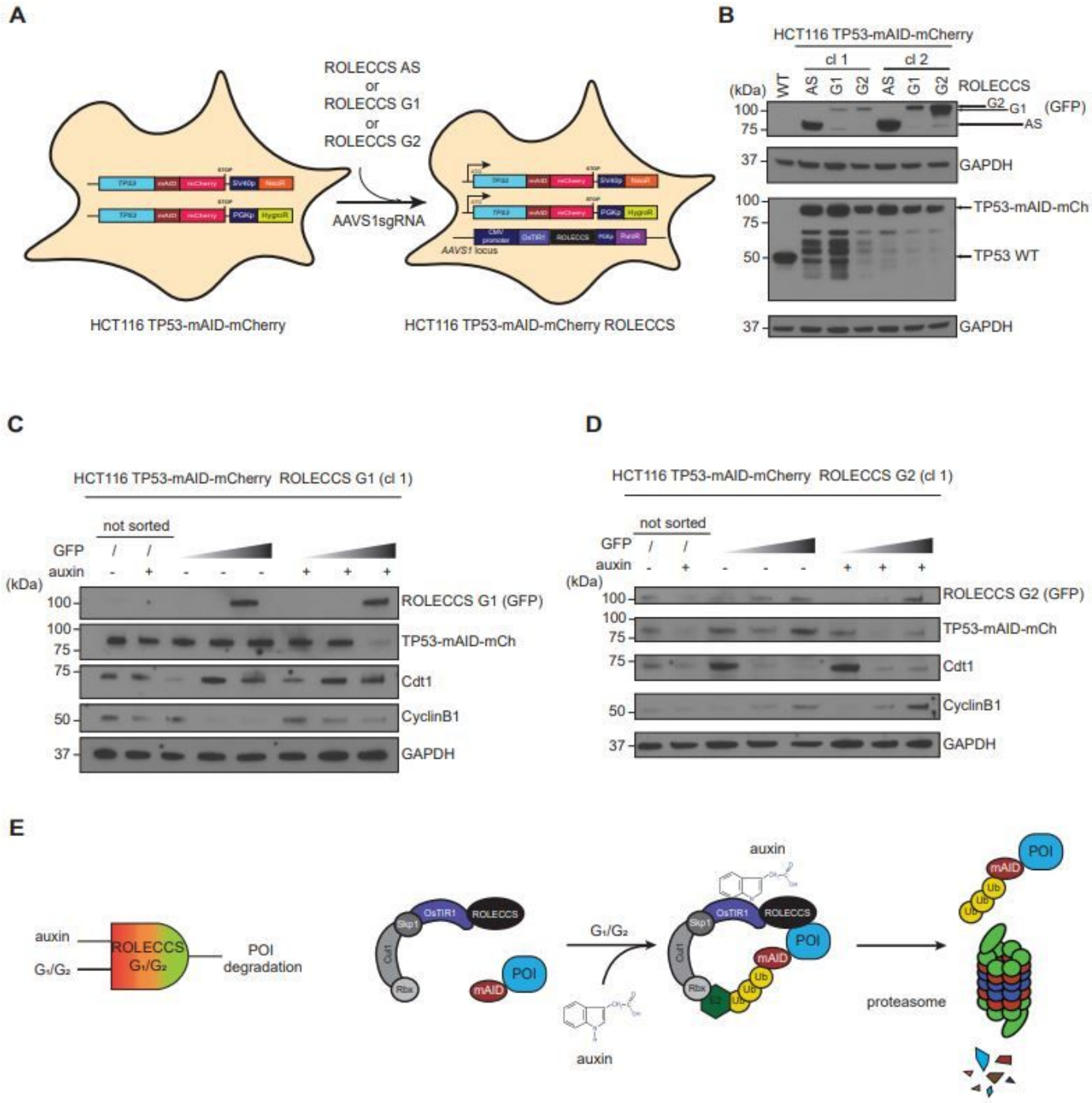

Figure 2

ROLECCS system downregulates endogenous proteins in a cell cycle-specific fashion. (**A**) Schematic illustration of the generation of HCT116 TP53-mAID-mCherry ROLECCS cells by introducing the transgenes ROLECCS (AS/G1/G2) at the safe-harbor *AAVS1* locus via CRISPR/Cas9 in HCT116 TP53-mAID-mCherry. (**B**) WB analysis of characterization of HCT116 TP53-mAID-mCherry with *AAVS1*-integrated ROLECCS variants (AS/G1/G2). ROLECCS AS, ROLECCS G1, and ROLECCS G2 were detected

using anti-GPF antibody (see arrows), TP53 wild type (WT) and TP53-mAID-mCherry (TP53-mAID-mCh) were detected using anti-TP53 antibody. GAPDH was used as loading control. HCT116 wild type (WT) were loaded for comparison. Two independent HCT116 TP53-mAID-mCherry ROLECCS clones (cl 1, cl 2) were analyzed. Images are representative of two independent experiments. (**C**) WB analysis of HCT116 TP53-mAID-mCherry *AAVS1*-edited with ROLECCS G1, clone 1 (cl 1) after sorting. Cells were treated with auxin or left untreated for one hour and then sorted for GFP intensity (ascending grey gradient triangle). Membrane was probed with anti-GFP antibody for ROLECCS G1 detection and mCherry antibody for TP53-mAID-mCherry (TP53-mAID-mCh) detection. Cdt1 and CyclinB1 were used as G_1 phase and G_2 phase specific markers, respectively. GAPDH was used as loading control. Not sorted (unsorted) cells were loaded for comparison. (**D**) WB analysis of HCT116 TP53-mAID-mCherry *AAVS1*-edited with ROLECCS G2, clone 1 (cl 1) after sorting. Treatments, sortings, and antibodies are the same as shown in panel E. Blots are representative of two independent experiments. (**E**) The ROLECCS system performs a Boolean logic computation. The contemporary presence of auxin and appropriate phase of the cell cycle are both simultaneously required to lead to targeted protein degradation. ROLECCS G1 and G2 are stable only through specific phases of the cell cycle (G_1/early S for ROLECCS G1, late S/G_2/M for ROLECCS G2), therefore their biological activity is restricted to those phases. However, auxin is required to trigger OsTIR1-mediated protein ubiquitylation, allowing proteasomal degradation of the POI only “on demand”, and only in the appropriate phase of the cell cycle.

Supplementary Files

This is a list of supplementary files associated with this preprint. Click to download.

- Supplemntaryvideo2.mp4
- CapeceetalSupplementaryInformation.docx
- SupplementaryVideo1.mp4
- SupplementaryVideo3.mp4
- CapeceetalFigures.pdf